'94 KACC (1994. 10. 17 ~ 20)

Extension of Shuster's algorithm for Spin-axis attitude and Sensor bias determination

No, Tae Soo
Koreasat Group, Korea Aeropsace Research Institute

위성 회전축 및 센서 바이어스 결정을 위한 확장 Shuster 알고리즘에 관한 연구

노 태 수
(항공우주연구소 선임연구원)

Abstract

Shuster's algorithm for spin-axis determination is extended to include sensor bias and mounting angle as its solve-for parameters. The relation between direct and derived measurements bias is obtained by linearizing their kinematic equations. A one-step least-square estimation technique referred to as the 'closed form' solution is used, and the solution provides a more refined and decent initial guess for the subsequent filtering process contained within the differential correction module. The modified algorithm is applied for attitude determination of a GEO communication satellite in transfer orbit, and its results are presented.

Introduction

Many satellites are spin-stabilized during part or all of their mission. For example, Koreasat will be spin-stabilized during its transfer orbit and 3-axis stabilized during its mission orbit.[1] Shown in Fig. 1 is the mission sequence of a typical GEO commnunication satellite. While in the transfer orbit, the orbit and attitude of the spacecraft are determined as accurately as possible and the spacecraft performs several attitude maneuvers such as spin-rate adjustment or spin-axis reorientation upon ground commands for the orbit insertion and Earth acquisition maneuver. In order to plan or evaluate its attitude maneuver, it becomes necessary to determine the spacecraft's attitude accurately before and after the maneuvers. Also hardware-related parameters such as sensor bias and mounting angle need to be correctly determined to make sure that they endured the launch environment and are performing as expected.

The well-established least-square estimation technique has been extensively used for this purpose.[2],[3]. One of its implementations is a differential correction scheme, which will iteratively determine the final attitude if it converges to the right solution. However, most differential correction scheme require a good initial guess which is sufficiently close to the solution. This is because the algorithm is inherently based upon the assumption of linearization. Wertz has developed several deterministic methods which use the right number of measurements.[4] Shuster used 'derived' measurements and obtained a one-step differential correction algorithm which does not need any initial guess.[5]

In case of Koreasat, one runs the attitude determination S/W module to process Sun sensor and Horizon sensor telemetry data which are downlinked to the ground station. First "Closed Form Solution (CF)" module, which is based on Shuster's algorithm, is run to obtain a decent initial guess for the following full-scale "Differential Correction (DC)" module. Although the CF module yields quite good results in the presence of a relatively small sensor bias, it is still possible that the CF module provides totally wrong information to the DC module because the CF algorithm does not include the sensor bias as its solve-for parameters.

Therefore the purpose of the present paper is to extend and improve Shuster's algorithm for the attitude and sensor bias determination of the spin-stabilized spacecraft, and verify it through extensive numerical simulation.

Measurements and Shuster's algorithm

Assuming that Sun and horizon sensors are measuring devices and assuming a torque-free motion, Fig. 2 describes the geometry of a typical measurement set used for the determination of spin-axis orientation as defined in Fig. 3. In Fig. 2, β, $\frac{\Omega}{2}$, and Φ denote direct measurements which are, respectively, Sun angle, half of Earth width, and Sun-Earth rotation angle. If we use $\underline{s}$, $\underline{e}$, and $\underline{a}$ to represent sun, nadir, and attitude (spin-axis) unit vectors, the following measuremet equations are obtained by using the spherical trigonometry. That is,

$$\beta = \cos^{-1}(\underline{s}\cdot\underline{a}) + \beta_B \qquad (1)$$

$$\frac{\Omega}{2} = \cos^{-1}\left[\frac{\cos\rho - \cos\eta\cos\gamma}{\sin\eta\sin\gamma}\right] + \Omega_B \qquad (2)$$

$$\Phi = \tan^{-1}\left[\frac{\underline{a}\cdot\underline{n}}{\underline{s}\cdot\underline{e} - (\underline{s}\cdot\underline{a})(\underline{e}\cdot\underline{a})}\right] + \Phi_B \qquad (3)$$

where ρ= Earth radius angle, $\cos\eta = \underline{a}\cdot\underline{e}$, $\underline{n} = \underline{s}\times\underline{e}$, γ= Horizon sensor mounting angle, and the subscript B denotes corresponding measurement bias. The orientation of attitude vector $\underline{a} = (a_1, a_2, a_3)^T$ is related to angles α(right ascension) and δ(declination) as can be noted from Fig.3,

$$a_1 = \cos\alpha\cos\delta$$
$$a_2 = \sin\alpha\cos\delta \qquad (4)$$
$$a_3 = \sin\delta$$

In Ref.[3], direct measurements as defined in Eqs. (1)-(3), are used to determine $\underline{x} = (\alpha, \delta, \beta_B, \Omega_B, \Phi_B, \gamma)^T$ iteratively.

Shuster's algorithm assumes no bias and uses "derived" measurement equations as follows.

$$c_{\beta_i} = \underline{s}_i\cdot\underline{a}$$
$$c_{\eta_i} = \underline{e}_i\cdot\underline{a} \qquad (5)$$
$$c_{\Phi_i} = \underline{n}_i\cdot\underline{a}$$

where $c_{\beta_i} = \cos\beta_i$, $c_{\eta_i} = \cos\eta_i$, $c_{\Phi_i} = \sin\beta_i\sin\eta_i\sin\Phi_i$, and i denotes the i^{th} measurement set. Then one may find $\underline{a}$ (insetad of α and δ) such that it minimizes the cost function,

$$J = \sum_{i=1}^{N}\{(c_{\beta_i} - \underline{s}_i\cdot\underline{a})^2/\sigma_{\beta_i}^2 + (c_{\eta_i} - \underline{e}_i\cdot\underline{a})^2/\sigma_{\eta_i}^2 + (c_{\Phi_i} - \underline{n}_i\cdot\underline{a})^2/\sigma_{\Phi_i}^2\} \qquad (6)$$

subject to the constraint $|\underline{a}|=1$. Readers are referred to Ref.[5] for further development.

Among other things, the beauty of the above method lies in the fact that it requires no initial guess for attitude vector $\underline{a}$, although a slight complication aries for the calculation of variances ($\sigma_{\beta_i}^2, \sigma_{\eta_i}^2, \sigma_{\Phi_i}^2$) of "derived" measurements from those of direct ones. Also nadir angle η needs to be determined by combining direct measurements. There are several methods for this purpose.[4]

Extension of Shuster's algorithm

With small biases, Shuster's algorithm yields a decent initial guess for the subsequent least square differential correction module, which will eventually determine the attitude and bias. However, if relatively large measurement bias are present, Shuster's algorithm may result in poor estimates. Then it will take more computing time and iteration to converge to the right solution.

One remedy to this problem is to include the measurement bias as a solve-for parameter. With bias correction, Eq. (5) may be written as

$$\cos(\beta_i - \beta_B) = \underline{s}_i\cdot\underline{a}$$
$$\cos(\eta_i - \eta_B) = \underline{e}_i\cdot\underline{a} \qquad (7)$$
$$\sin(\beta_i - \beta_B)\sin(\eta_i - \eta_B)\sin(\Phi_i - \Phi_B) = \underline{n}_i\cdot\underline{a}$$

Assuming that the bias is small enough, Eq.

(7) may be rewritten as

$$c_{\beta_i} = \underline{s}_i \cdot \underline{a} - \beta_B \sin\beta_i$$

$$c_{\eta_i} = \underline{e}_i \cdot \underline{a} - \eta_B \sin\eta_i \qquad (8)$$

$$c_{\Phi_i} = \underline{n}_i \cdot \underline{a} + \beta_B \cos\beta_i \sin\eta_i \sin\Phi_i + \eta_B \sin\beta_i \cos\eta_i \sin\Phi_i + \Phi_B \sin\beta_i \sin\eta_i \cos\Phi_i$$

In Eq. (8) β_B and Φ_B are bias for direct measurements as can be seen from Eqs. (1)-(3), but η_B is not.

Referring to Fig. 2, one uses spherical trigonometry to write

$$\cos\rho = \cos\gamma\cos\eta + \sin\gamma\sin\eta\cos(\frac{\Omega}{2}) \qquad (9)$$

$$\cos\psi = \cos\beta\cos\eta + \sin\beta\sin\eta\cos\Phi \qquad (10)$$

One may solve for nadir angle η using either Eq. (9) or (10) with the constraint,

$$\cos\eta^2 + \sin\eta^2 = 1 \qquad (11)$$

However this approach will result in multiple solutions and the sign ambiguity should be resolved. Shuster suggested that Eqs. (9) and (10) be simultaneously solved for $\sin\eta$ and $\cos\eta$ to give

$$\eta = \tan^{-1}\left(\frac{\sin\eta}{\cos\eta}\right) = \tan^{-1}\left(\frac{\cos\psi\cos\gamma - \cos\rho\cos\beta}{-\cos\psi\sin\gamma\cos\frac{\Omega}{2} + \sin\beta\cos\Phi\cos\rho}\right) \qquad (12)$$

However Eqs. (9) and (10) may not be satisfied due to measurement errors. Therefore, if $\sin\eta$ and $\cos\eta$ obtained from Eqs. (9) and (10) violate the constraint, Eq. (11), too much, that particular data set should be discarded.

With the bias-corrected measurements (if there are any), such a data set is more likely to statisfy Eqs. (9) and (10), and Eq. (12) may be modified to

$$\tan(\eta-\eta_B) = \frac{\cos\psi\cos\gamma - \cos\rho\cos(\beta-\beta_B)}{-\cos\psi\sin\gamma\cos(\frac{\Omega}{2}-\Omega_B) + \sin(\beta-\beta_B)\cos(\Phi-\Phi_B)\cos\rho} \qquad (13)$$

Similar to bias-corrected measurement equations, one may linearize Eq. (13) using the assumption of small bias and assert that error contributed from bias on both sides be equal. This will result in,

$$\eta_B = k_1\beta_B + k_2\Omega_B + k_3\Phi_B \qquad (14)$$

where $k_1 = -(\cos\rho\sin\beta\cos\psi\sin\gamma\cos\frac{\Omega}{2} + \cos\psi\cos\gamma\cos\beta\cos\Phi\cos\rho - \cos^2\rho\cos\Phi)/\Delta^2$

$k_2 = -(\cos\psi\cos\gamma - \cos\rho\cos\beta)\cos\psi\sin\gamma\sin\frac{\Omega}{2}/\Delta^2$,

$k_3 = (\cos\psi\cos\gamma - \cos\rho\cos\beta)\sin\beta\sin\Phi\cos\rho/\Delta^2$,

$\Delta = (-\cos\psi\sin\gamma\cos\frac{\Omega}{2} + \sin\beta\cos\Phi\cos\rho)/\cos\eta$

If Eq. (14) is substituted into Eq. (8) and the resulting equation is used to rewrite Eq. (6), then we obtain

$$J = \sum_{i=1}^{N}(\underline{y}_i - H_i\underline{x})^T W_i (\underline{y}_i - H_i\underline{x}) \qquad (15)$$

where $\underline{y}_i = (c_{\beta_i}, c_{\eta_i}, c_{\Phi_i})^T$, $\underline{x} = (\underline{a}^T\ \beta_B\ \Omega_B\ \Phi_B)^T$

$$H_i = \begin{bmatrix} \underline{s}_i^T & -\sin\beta_i & 0 & 0 \\ \underline{e}_i^T & h_{24} & h_{25} & h_{26} \\ \underline{n}_i^T & h_{34} & h_{35} & h_{36} \end{bmatrix}$$

$$h_{2,(3+j)} = -\sin\eta_i k_j,\ j=1,2,3$$

$$h_{34} = \cos\beta_i\sin\eta_i\sin\Phi_i + k_1\sin\beta_i\cos\eta_i\sin\Phi_i,$$

$$h_{35} = k_2\sin\beta_i\cos\eta_i\sin\Phi_i$$

$$h_{36} = \sin\beta_i\sin\eta_i\cos\Phi_i + k_3\sin\beta_i\cos\eta_i\sin\Phi_i$$

$$W_i = \begin{bmatrix} \frac{1}{\sigma_{\beta_i}^2} & 0 & 0 \\ 0 & \frac{1}{\sigma_{\eta_i}^2} & 0 \\ 0 & 0 & \frac{1}{\sigma_{\Phi_i}^2} \end{bmatrix}$$

Note that the solve-for state vector $\underline{x}$ is extended to include sensor bias and any reference to or initial guess of the solve-for state vector $\underline{x}$ is not required to evaluate the matrix H_i. To this parameter estimation problem one may apply the 'usual' batch estimation algorithm. More details may be found in Ref. [5].

Simulation and numerical example

To show and validate the usefulness of the current extension to Shuster's original algorithm, extensive simulation has been performed. A simulated measurement data set has been generated using a known solution and Gaussian noise with various levels of measurement bias. The attitude and orbit are assumed to be torque-free and two-body Keplerian, respectively. Table 1 shows the true solution and noise characteristics.

Shown in Table 2 is a typical example from which one may notice that the extended algortihm yields good estimates of sensor bias. In Figs. (4)-(6), the z-axis denotes error in attitude estimates $[\sqrt{(\alpha-\alpha_{true})+(\delta-\delta_{true})}]$ and the x- and y-axes are the corresponding sensor bias used for the simulated data set. And the upper and lower surfaces, respectively, correspond to results from Shuster's and the extended algorithms. It is apparent from Figs. (4)-(6) that the extended algorithm tends to result in more accurate estimates of the attitude than Shuster's in the presence of a moderate range of sensor bias. However, both algorithms yield poor estimates for the extreme situation.

Conclusion

Shuster's algorithm is further developed so that it can be used to obtain estimates of spin-axis attitude and sensor bias as well. Numerical simulation shows that the extended algorithm yields more accurate estimates of attitude than Shuster's. The results may be used as a more decent initial guess to the subsequent estimation program such as differential correction.

Acknowledgement

This work is partially supported from Korea Telecom and the author would like to thank Mr. I.S. Son and Mr. J.E. Lee for preparing plots and proof reading.

Referenecs

1. ______ KOREASAT System Proposal, Vol. III, Book 1, GE Technical Services Company, Inc., July 22, 1991

2. Markley, F. M., "Attitude Determination and Parameter Estimation Using Vector Observation: Theory," The Journal of the Astronautical Sciences, Vol. 37, No. 1, January-March 1989.

3. No, T. S., and S. K., Kim, "Koreasat Orbit and Attitude Determination during Transfer Orbit," The Korean Society for Aeronautical and Space Sciences, Spring Conference, 1994

4. Wertz, J. R. (editior), Spacecraft Attitude Determination and Control, D. Reidel Publishing Company, 1978.

5. Shuster, M., "Efficient Algorithm for Spin-axis Attitude Estimation," The Journal of the Astronautical Science, Vol. 31, No. 2, April-June 1983.

Table 1. Characteristics of simulated data set

True attitude	α_{true} = 105.48 deg., δ_{true} = -8.39 deg.		
Transfer orbit elements	semi-major = 24947.5 Km Eccentricity = 0.6901 Right ascension of ascensding node = 149 deg. Argument of perigee = 358 deg. Inclination = 20.39 deg.		
No. of measurement		778	
Noise statistics		Mean(deg.)	Variance
	β	-8×10^{-3}	0.32
	Ω	2×10^{-2}	0.34
	Φ	2×10^{-2}	0.29

Table 2. Example of sensor bias estimation

Solve for variables	True value	Shuster algorithm	Extended algorithm
α(deg.)	105.48	110.11	104.88
δ(deg.)	-8.39	-5.09	-7.88
β_B(deg.)	5.0	N/A	5.58
Ω_B(deg.)	-5.0	N/A	-6.59
Φ_B(deg.)	5.0	N/A	5.86

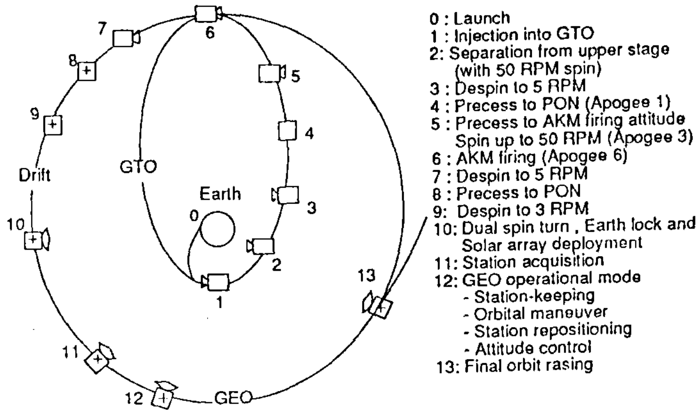

Fig 1. Launch Sequence of a Typical GEO Satellite

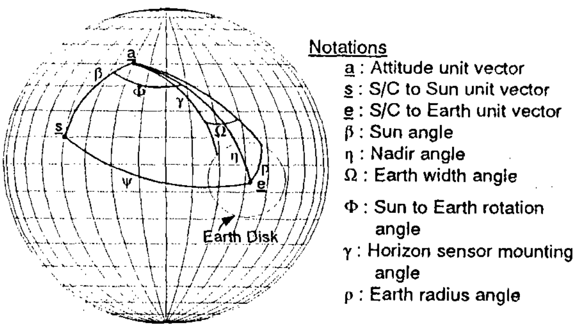

Fig 2. Measurement geometry

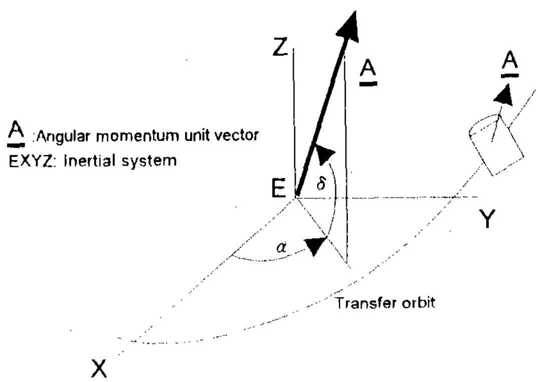

Fig. 3 Spin-axis attitude vector

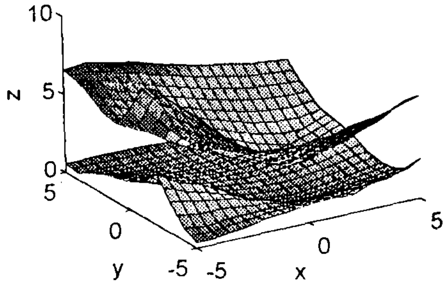

Fig. 4 Simulation results
($x= \beta_B$, $y= \Omega_B$, $\Phi_B=3$ deg.)

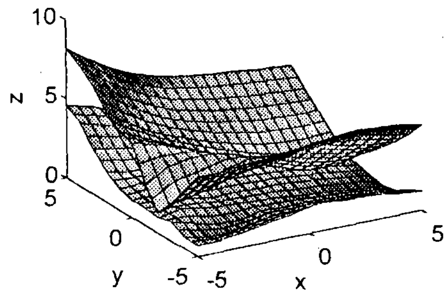

Fig. 5 Simulation results
($x= \beta_B$, $y= \Phi_B$, $\Omega_B=3$ deg.)

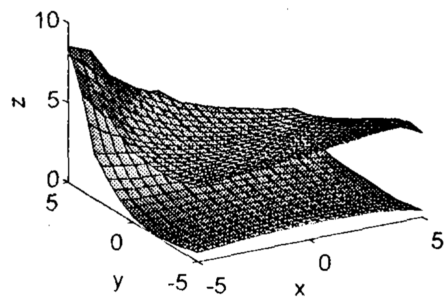

Fig. 6 Simulation results
($x= \Omega_B$, $y= \Phi_B$, $\beta_B=3$ deg.)